Journal of Atmospheric and Solar-Terrestrial Physics 165-166 (2017) 25–37

Contents lists available at ScienceDirect

Journal of Atmospheric and Solar-Terrestrial Physics

journal homepage: www.elsevier.com/locate/jastp

Aliasing of the Schumann resonance background signal by sprite-associated Q-bursts

Anirban Guha [a,b,*], Earle Williams [b], Robert Boldi [c], Gabriella Sátori [d], Tamás Nagy [d], József Bór [d], Joan Montanyà [e], Pascal Ortega [f]

[a] Department of Physics, Tripura University, Tripura, India
[b] Parsons Laboratory, Massachusetts Institute of Technology, Cambridge, MA, USA
[c] College of Natural and Health Sciences, Zayed University, Dubai, United Arab Emirates
[d] Research Centre for Astronomy and Earth Sciences, GGI, Hungarian Academy of Sciences, Sopron, Hungary
[e] Electrical Engineering Department, Polytechnic University of Catalonia, Barcelona, Spain
[f] Laboratory GEPASUD, University of French Polynesia, Tahiti, French Polynesia

ARTICLE INFO

Keywords:
Schumann resonances
Transient Luminous Events (TLEs)

ABSTRACT

The Earth's naturally occurring Schumann resonances (SR) are composed of a quasi-continuous background component and a larger-amplitude, short-duration transient component, otherwise called 'Q-burst' (Ogawa et al., 1967). Sprites in the mesosphere are also known to accompany the energetic positive ground flashes that launch the Q-bursts (Boccippio et al., 1995). Spectra of the background Schumann Resonances (SR) require a natural stabilization period of ~10–12 min for the three conspicuous modal parameters to be derived from Lorentzian fitting. Before the spectra are computed and the fitting process is initiated, the raw time series data need to be properly filtered for local cultural noise, narrow band interference as well as for large transients in the form of global Q-bursts. Mushtak and Williams (2009) describe an effective technique called Isolated Lorentzian (I-LOR), in which, the contributions from local cultural and various other noises are minimized to a great extent. An automated technique based on median filtering of time series data has been developed. These special lightning flashes are known to have greater contribution in the ELF range (below 1 kHz) compared to general negative CG strikes (Huang et al., 1999; Cummer et al., 2006). The global distributions of these Q-bursts have been studied by Huang et al. (1999) Rhode Island, USA by wave impedance methods from single station ELF measurements at Rhode Island, USA and from Japan Hobara et al. (2006). The present work aims to demonstrate the effect of Q-bursts on SR background spectra using GPS time-stamped observation of TLEs. It is observed that the Q-bursts selected for the present work do alias the background spectra over a 5-s period, though the amplitudes of these Q-bursts are far below the background threshold of 16 Core Standard Deviation (CSD) so that they do not strongly alias the background spectra of 10–12 min duration. The examination of one exceptional Q-burst shows that appreciable spectral aliasing can occur even when 12-min spectral integrations are considered. The statistical result shows that for a 12-min spectrum, events above 16 CSD are capable of producing significant frequency aliasing of the modal frequencies, although the intensity aliasing might have a negligible effect unless the events are exceptionally large (~200 CSD). The spectral CSD methodology may be used to extract the time of arrival of the Q-burst transients. This methodology may be combined with a hyperbolic ranging, thus becoming an effective tool to detect TLEs globally with a modest number of networked observational stations.

1. Introduction

It is known that the background and transient activity in Schumann Resonances (SR) are physically linked (Williams et al., 1999). However, it is not completely known how ELF transients affect the background SR spectra within a stabilization period of several minutes. Mushtak and Williams (2011), Mushtak et al. (2012) and Guha et al. (2014) described how the background SR modal parameters could be sanitized by a method called Core Standard Deviation (CSD) by rejecting the time series in short segments containing the Q-bursts (see Methodology section

* Corresponding author. Department of Physics, Tripura University, Tripura, India.
E-mail address: anirban1001@yahoo.com (A. Guha).

https://doi.org/10.1016/j.jastp.2017.11.003
Received 29 April 2017; Received in revised form 28 October 2017; Accepted 2 November 2017
Available online 4 November 2017

below for details) (Ogawa et al. 1967; Boccippio et al. 1995). These special lightning flashes are known to have greater contribution in the ELF range (below 1 kHz) compared to general negative CG strikes (Huang et al. 1999; Cummer et al. 2006; Hobara et al. 2006). The CSD method can also be used to filter out the local cultural noise that can spoil the background SR spectra. The motivation of this work is to investigate whether one ELF transient from a positive lightning stroke (Q-burst) and local cultural noise has sufficient energy to alias the background spectra by modifying its background spectral shape within a given time period.

When using SR electromagnetic observations for monitoring global background lightning activity, it is essential to sanitize the experimental recordings from any non-background elements, even though the actual data to be used in such an inversion problem are the resonance characteristics: namely intensity, frequency, and quality factor of several lowest order SR modes (Mushtak et al., 2010). The sanitizing requirement makes it necessary to start the processing directly with the initial time series.

Obvious noise sources are local interferences of various kinds: external man-made, weather-related, and internal equipment-related. These elements can be relatively easily identified and eliminated. Other sources of noise are of a less obvious nature. In this category are transients, strong signatures produced by intense lightning discharges whose impulsive signatures dwarf the background amplitudes. Since the transients are of the same lightning origin as the background component, there is a temptation to include their parent discharges into the background ensemble as its high-energy "tail". However, these transients are easily capable of aliasing the background spectral signature, since they contain information on their spatial origin that differs from that in the background spectra (Nickolaenko et al., 2010; Price, 2016).

2. Data selection for the present study: Q-bursts for sprite events in Spain

For the present study, 4 kHz-sampled ELF data in the SR band from West Greenwich, Rhode Island (RI), USA (41.6°N,-71.7°W) are used along with video camera observations of sprites from the Ebro Delta in northeastern Spain (42.94°N, 0.14°E). A map of the observational stations showing the Great Circle Distance (GCP) between them is shown in Fig. 1.

The ELF system in RI consists of two induction coil magnetic field sensors horizontally orientated along the geographical East-West and North-South direction and one vertical electric field sensor. Both the magnetic and electric field sensors have a flat band pass within the frequency range 1–100 Hz. We use only vertical electric field ELF data for the present work.

The Sprites are recorded at 25 interlaced images per second by Watec 902H type cameras with light-sensitive 1/2 inch charge coupled device (CCD) sensors with 12mm F0.8 lenses (31° angle of view) and UFO-Capture event detection software (van der Velde et al., 2014). The peak currents of the sprite producing lightning data are provided by the LINET (LIghtning NETwork) very low frequency and low frequency (1–200 kHz) time-of-arrival network (Betz et al., 2004).

The data from the World Wide Lightning Location Network (WWLLN) are also used to identify the parent strokes for the sprites and their average VLF energy (Hutchins et al., 2012). All the data are time stamped in UT using GPS synchronization. Initially, 35 sprite events were selected spread over 8 days from the years 2011–2013. Out of the 8 days, 6 days of ELF data were available from RI. 21 possible ELF events were identified from the ELF time series data that could have possible correlation with the causative Q-burst lightning near the Ebro Delta. Out of these 21 events, 9 events were selected to search for the causative strokes from the WWLLN data base. Based on the average energy of the parent Q-burst identified from the WWLLN data, the three most powerful strokes were considered for final analysis in the present work. The parameters for the three selected events are furnished in Table 1.

3. Methodology of cleaning background time series

To demonstrate local interference and estimate the effect of the transients on the background SR parameters, we examine observations from two stations: "BLK" (Belsk, Poland) and "NCK" (Nagycenk, Hungary), separated by a small distance of about 550 km (this distance is small only in terms of the global Schumann resonances). Such simultaneous observations provide an opportunity to exclude local interference and to estimate the transients' effect on the background SR parameters. The initial experimental material (Fig. 2) is presented in 12-min intervals, further called "periods" from the initial time series of vertical electric field registered at both stations during ten days in January 2009.

To identify the presence of contaminating elements, each 12-min period is subdivided into 144 time intervals of 5 s duration, hereafter

Fig. 1. Map of the ELF observation site in Rhode Island, USA and the sprite observation site in Ebro Delta, Spain. The Great Circle Path (GCP) distance between the two experimental sites is 5.4 Mm.

Table 1
The sprite and WWLLN parameters for three selected ELF events on 20th November, 2011.

Sprite detection time (UT) hh:mm:ss.sss	Sprite latitude (Degree)	Sprite longitude (Degree)	peak current (kA)	WWLLN detection time (UT) hh:mm:ss.ssss	WWLLN latitude (Degree)	WWLLN longitude (Degree)	WWLLN average energy (kJ)	WWLLN energy uncertainty (kJ)
03.35.51.289	40.88	0.65	+51	03.35.51.2893	41.10	0.57	32	13
03.42.50.711	40.88	0.65	+49	03.42.50.7118	40.92	0.73	120	72
03.49.07.085	40.99	0.53	+122	03.49.07.086	40.96	0.55	59	32

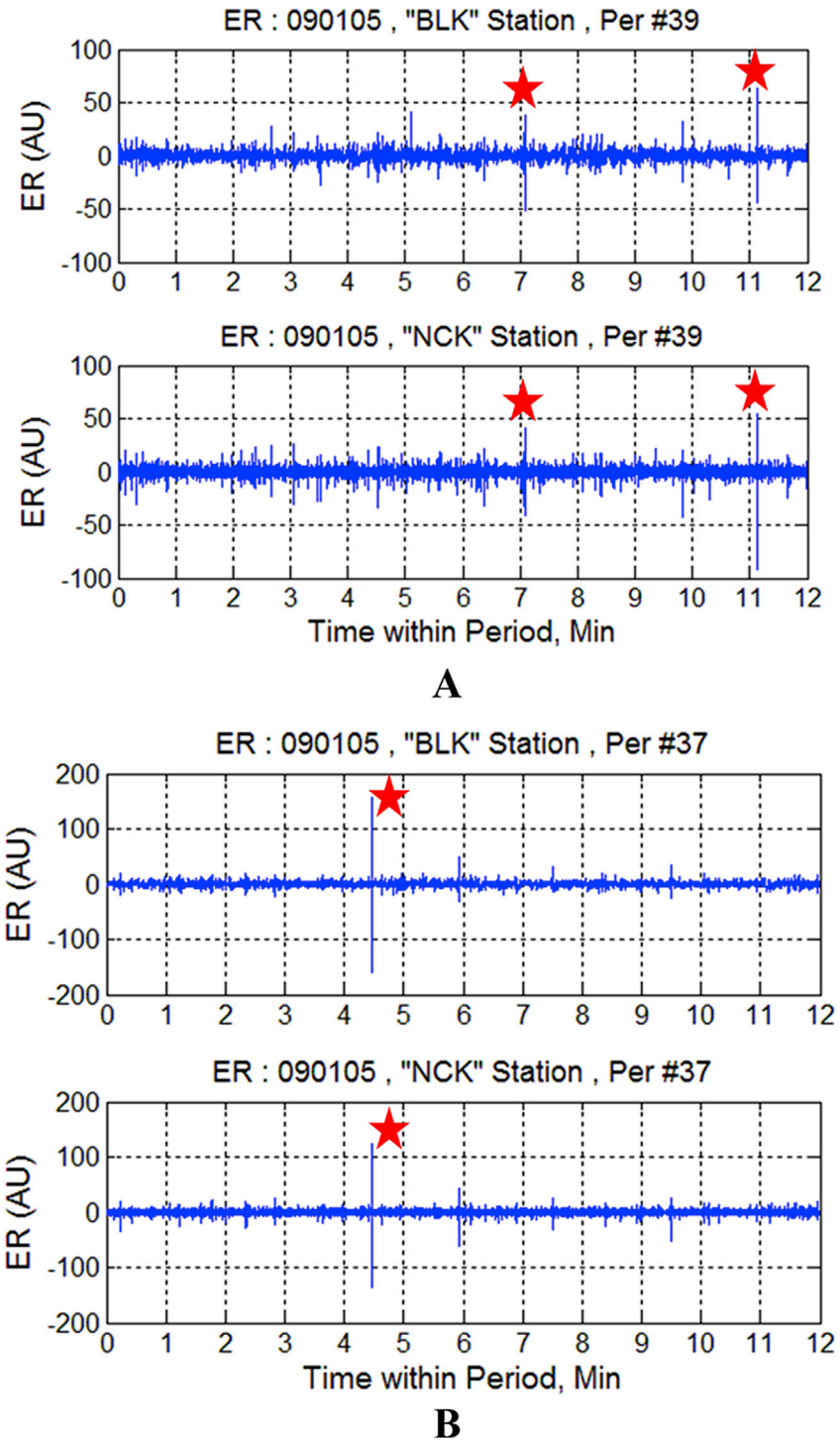

Fig. 2. Examples of 12-min time series of the vertical electric field registered simultaneously at two "ELF-close" locations Belsk (BLK), Poland and Nagycenk (NCK), Hungary and containing: (A) two medium transients (B) a very-strong transient signature. The transients are marked with red stars. (For interpretation of the references to colour in this figure legend, the reader is referred to the web version of this article.)

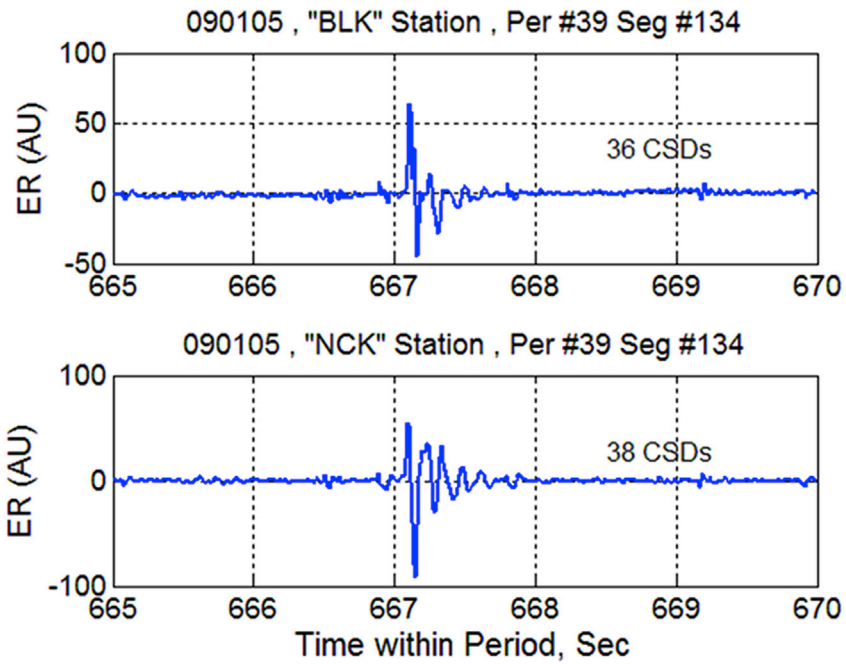

A

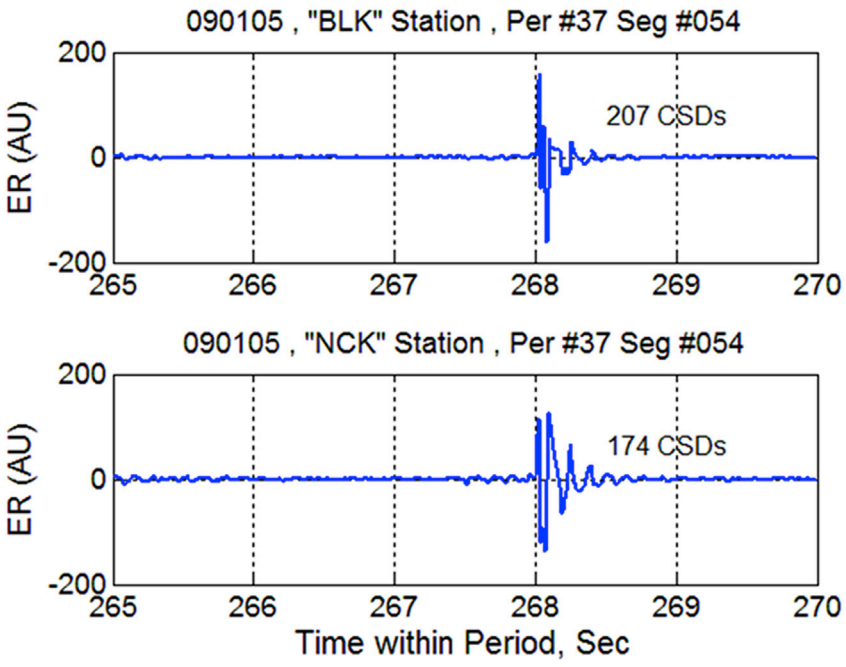

B

Fig. 3. Examples of a medium transient (A) and a very-strong transient (B) registered simultaneously at two "ELF-close" locations (Belsk and Nagycenk) within 5-sec segments.

called "segments". One such segment containing a transient is shown in Fig. 3. For each segment, the Spectral Power Density (SPD) is calculated and integrated over the first four SR modes into the Spectral Power Content (SPC). The histogram of the SPCs (Fig. 4) for the given period is analyzed. Basically, the SPC is the area under the spectrum produced by the FFT procedure.

The general form of the SPC histograms is a "core" distribution (the corresponding range of SPC is marked by horizontal magenta line segments in Fig. 4 and is associated mainly with the background contribution). The core of the distribution is determined by the rule when there are at least three null segments (segments with no contribution) after any non-zero SPC segment in the histogram. Additional segments of the

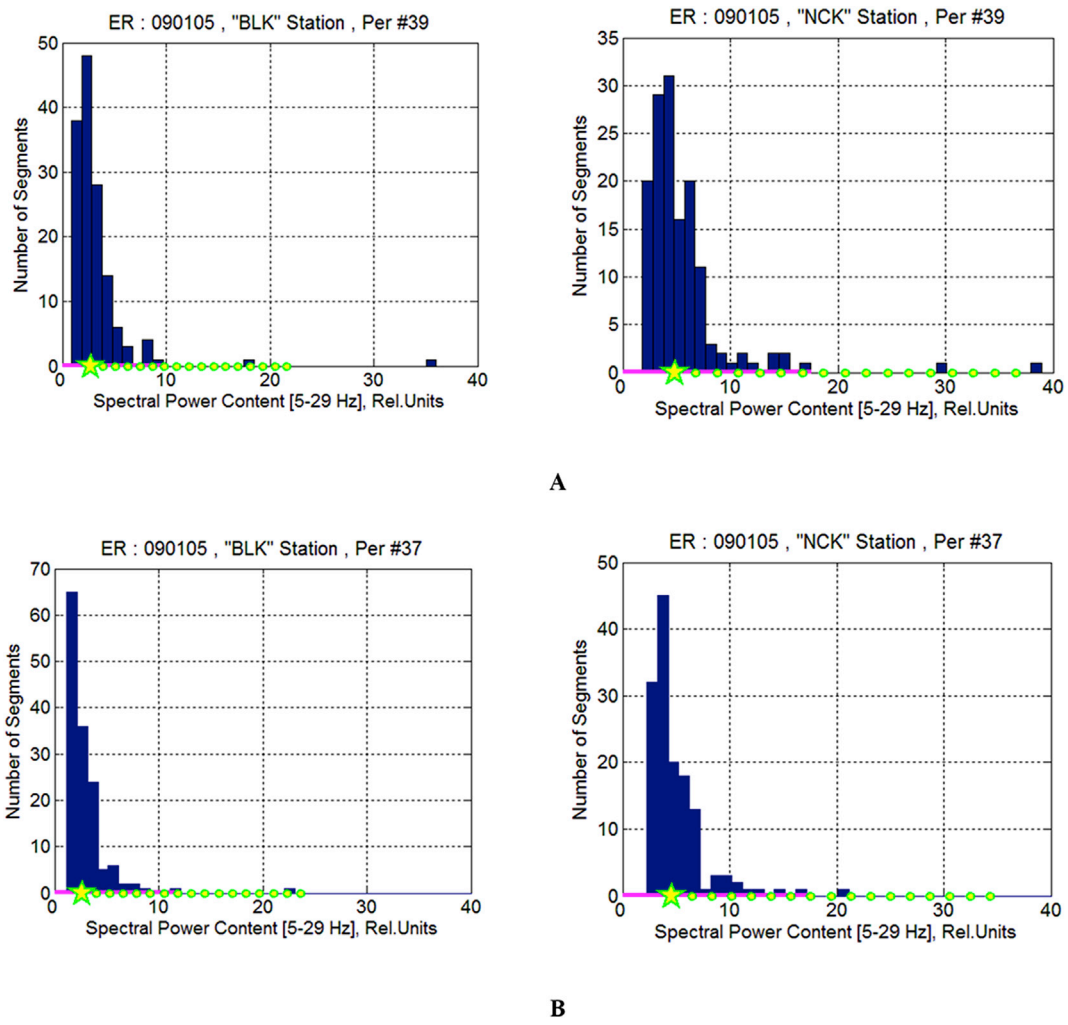

Fig. 4. Examples of histograms of spectral power content from 12 min (144 5-sec segments) data segments in Fig. 1 for Belsk (BLK) and Nagycenk (NCK) for period #39 (A) and #37 (B). The core distributions are indicated by horizontal magenta lines. The core averages and corresponding standard deviations are denoted by stars and circles, respectively. The core of the distribution is determined by the rule when there are at least three null segments (segments with no contribution) after any non-zero Spectral Power Content (SPC) each withthin 5-sec segments in the histogram.

histogram also appear with SPC of questionable origin from the "background" point of view. To investigate this "tail", the core mean value (CMV, identified by stars in Fig. 4) and multiples of the Core Standard Deviation (CSD) of the core distribution are computed and identified by circles in Fig. 4.

The stabilization diagrams in Fig. 5 show the dependence of the SR parameters on the threshold, expressed in CSDs. The contributions of the segments with SPCs beyond the threshold are eliminated to compute the SR parameters for the stabilization diagrams. The general form of a stabilization diagram shows an initial portion where the background is underrepresented since significant portion of the core distribution (marked by magenta line in Fig. 4) is eliminated, due to which the SR parameters vary within this portion of the diagram. In the figures, Δfn are the deviations for the nth SR mode frequency computed over a 12-min period between a 16 CSD sanitation threshold and any other CSD threshold. The 'stabilization interval' means $\Delta f_n = 0$. P_n are the estimated power spectral density of different modes in arbitrary relative units within the range, $f_1 = 7.3–8.3$ Hz, $f_2 = 13.3–14.8$ Hz, $f_3 = 18.6–21$ Hz and $f_4 = 25.4–27.5$ Hz, where 'f' is the modal frequency over a 12-min period. Here the SPC in terms of the CSD threshold is running along the x-axis of the figures. The initial portion (left hand side of the horizontal line with $\Delta f_n = 0$) is followed by the proper stabilization interval ($\Delta f_n = 0$), where the background is presented to its full extent; and then, sometimes, by the destabilization interval due to the presence of the non-background elements (both local disturbances and transients) that do distort the previously stabilized SR parameters (right hand side of the horizontal line with $\Delta f_n = 0$). In Fig. 5, the pentagrams (5-pointed stars) show unsanitized (raw) SR parameters when the thresholds in SPC are extended to the largest values used in the analysis.

In Fig. 6 stabilization intervals are shown for the same day of January 2009 from the "BLK" and "NCK" locations. A definite correlation between stations can be seen. These plots as well as the results for other days and stations show that the threshold of 16 CSDs is, as a rule, located within the stabilization interval. An event originating from either cultural noise or from a large natural Q-burst transient in a segment with SPC beyond this threshold is causing a distortion of SR parameters and so is to be considered a non-background element, and accordingly needs to be eliminated.

The distorting effect of local interference is usually evident and besides, can be eliminated by simply comparing the SPCs from two "ELF-close" stations. In contrast, the influence of a transient event may be more subtle and the record cannot be sanitized by this comparison procedure. Nevertheless, "the rule of 16 CSDs", despite the empirical nature of both the CSD and the rule itself, is efficiently working for the transient events as well, whether they be medium (period #39) or very-strong (period #37) events. As a result, the 16 CSDs threshold can be accepted as a "frontier" between the background and transient global lightning populations.

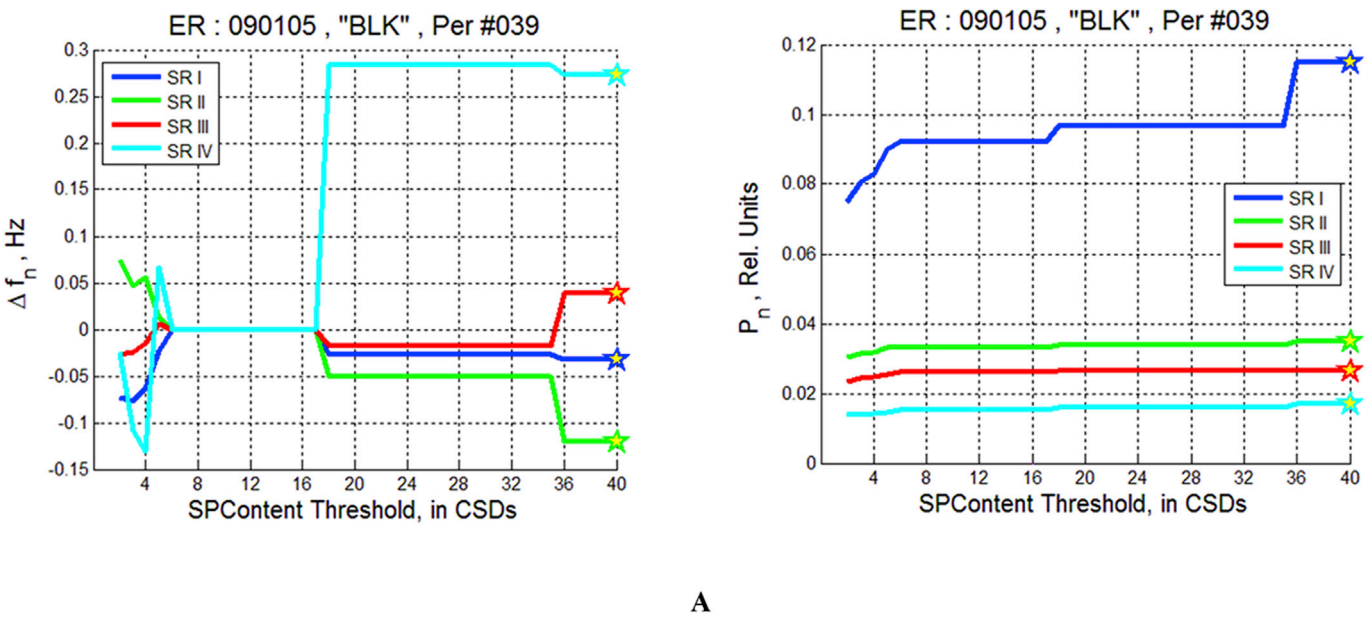

Fig. 5. The stabilization diagrams involving two measurables for period #039 (A) and #037 (B) on January 05, 2009 for station Belsk. The pentagrams show the un-sanitized (raw) SR parameters. Δfn are the deviations for the nth SR mode frequency computed over a 12-min period between a 16 CSD sanitation threshold and any other CSD threshold. P_n are the estimated power spectral density of different modes in arbitrary relative units within the range, $f_1 = 7.3–8.3$ Hz, $f_2 = 13.3–14.8$ Hz, $f_3 = 18.6–21$ Hz and $f_4 = 25.4–27.5$ Hz, where 'f' is the modal frequency over a 12-min period. The left hand portion of the stabilization diagram is followed by the proper stabilization interval (Δf_n), where the background is presented to its full extent. The right hand portion of the stabilization diagram indicates the presence of the non-background elements (both local disturbances and transients) that distort the stabilized SR parameters.

4. Observational results

The three selected sprite events for the present study and corresponding ELF time series are shown in Fig. 7a, b and 7c. The observed sprite from the Ebro Delta is shown in the upper panel in each case. In the lower panel, the ELF time series from RI is plotted for each case. The red line indicates the time of occurrence of the sprite as taken from the video camera. Note the finite time delay of 20–25 ms between the occurrence of the sprite and the peak Ez amplitude of the ELF transient detected at the RI station. This repeatable delay time is consistent with the ELF propagation speed along the great circle path between the causative Q-burst origin in the Ebro Delta and the RI station having a great circle distance of 5.4 Mm. The propagation speed of the electromagnetic wave estimated from the finite time delay is near 0.9c, 'c' being the speed of light in free space. The initial excursions of all three events are positive, indicative of positive charge transfer to ground in each case.

The temporal correlation of the WWLLN-measured VLF energy (Hutchins et al., 2013) of the sprite related Q-burst is shown in Fig. 8a, b and 8c for a 5-s time segment containing the ELF transient. The average energies of the three Q-burst events are 32, 120 and 59 kJ respectively. The black ellipse highlights the most energetic WWLLN stroke within the selected time interval and that corresponds to the sprite-producing Q-burst. The LMA observed peak currents for the three events are +51 kA, +49 kA and +122 kA respectively and shown in Table 1. The CSD values for the 5-s segments of the three selected Q-bursts events are 1.5, 1.2 and 2.9 respectively.

The background spectrum is computed for a 5-s segment without the transient and one additional second with the transient included so that the total segment length becomes 6 s. The results are shown in Fig. 9a to Fig. 9c. In all the cases, we exclude the third mode from analysis as it is

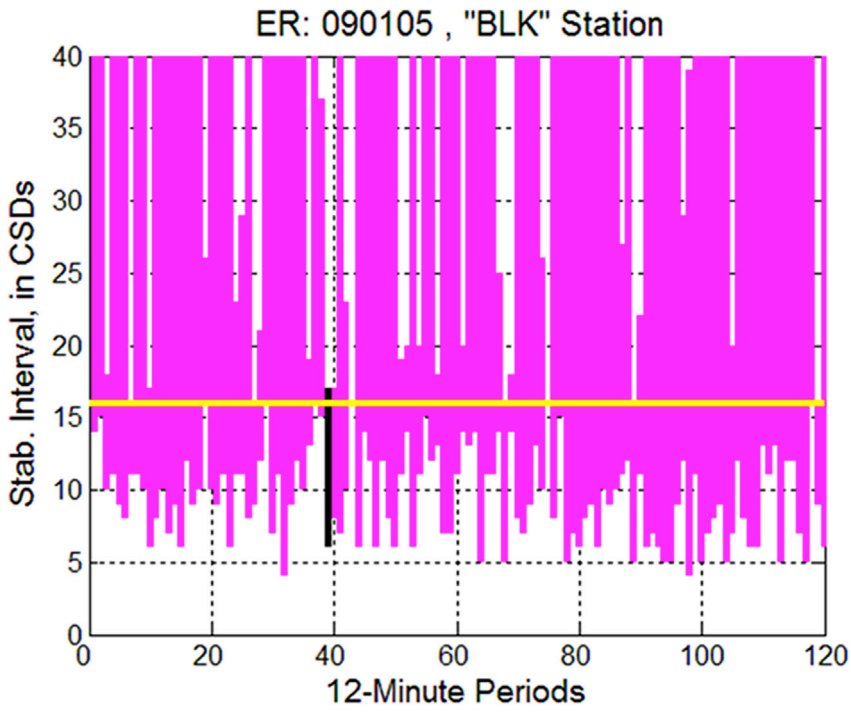

A

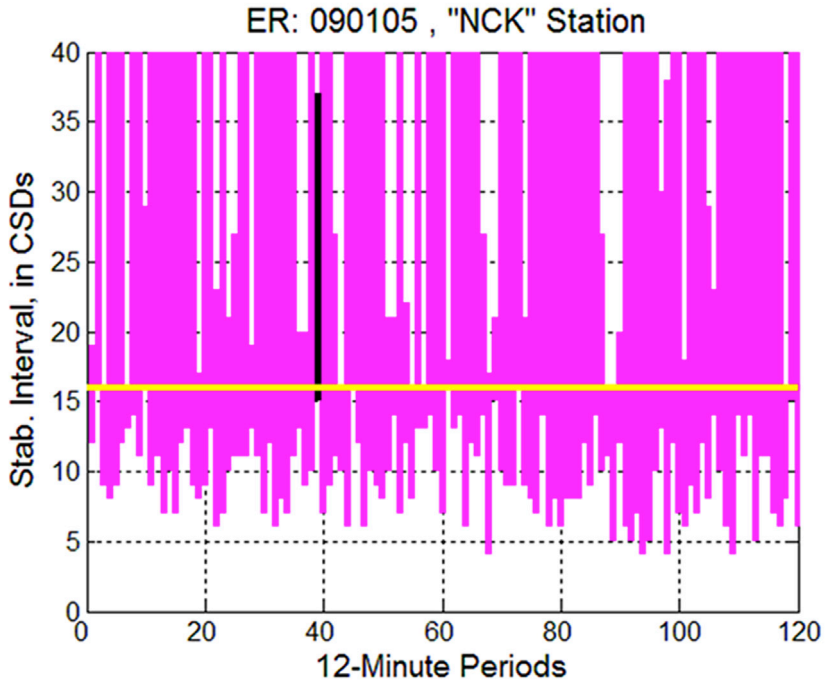

B

Fig. 6. Stabilization intervals vs. 12-minute period for electric SR observations at two "ELF-close" locations, Belsk (A) and Nagycenk (B). A definite correlation between the stations can be seen. The stabilization interval of 6–17 CSD for BLK station for period 39 (Fig. 5) is shown as a black vertical line in the upper panel. The stabilization interval for the same period for the NCK station is also shown in the lower panel. The 16 CSD line is shown as a yellow horizontal line. These plots as well as the results for other days and stations show that the threshold of 16 CSDs is, as a rule, located within the stabilization interval. (For interpretation of the references to colour in this figure legend, the reader is referred to the web version of this article.)

contaminated by 20 Hz interference.

Fig. 9a shows that due to the transient, the first mode PSD becomes ~50% larger (red color PSD) than the background value (blue color PSD). Higher order modes above the third mode exhibit greater PSD compared to the background spectra. Fig. 9b shows the results from the second event. The second mode shows a shift in frequency and

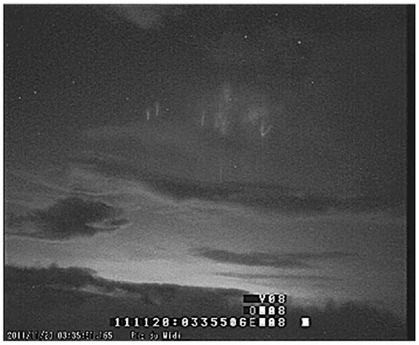

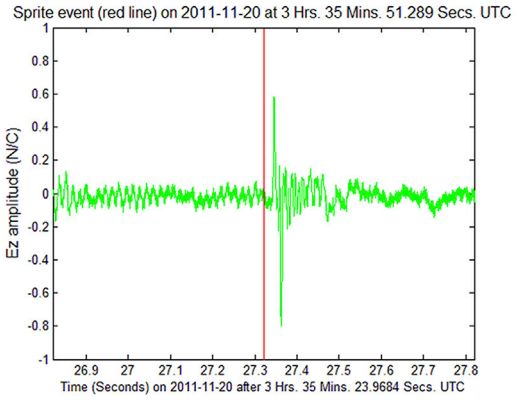

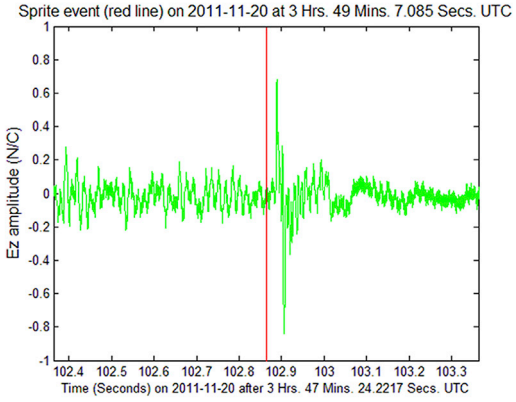

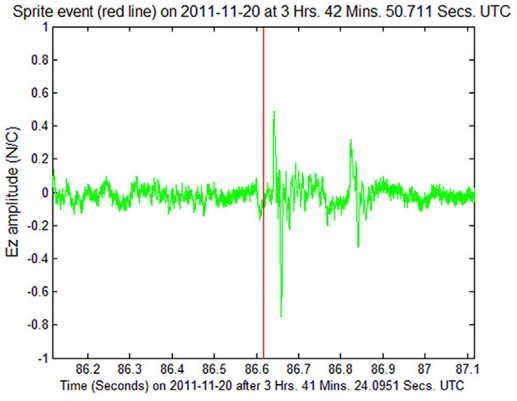

Fig. 7. a: The sprite event at 3 Hours 35 Minutes 51.289 Seconds UT and corresponding ELF time series from Rhode Island. The red line indicates the time of occurrence of the sprite event. The Ez amplitude is uncalibrated. b: The sprite event at 3 Hours 42 Minutes 50.711 Seconds UT and corresponding ELF time series from Rhode Island. The red line indicates the time of occurrence of the sprite event. The Ez amplitude is uncalibrated. c: The sprite event at 3 Hours 49 Minutes 07.085 Seconds UT and corresponding ELF time series from Rhode Island. The red line indicates the time of occurrence of the sprite event. The Ez amplitude is uncalibrated. (For interpretation of the references to colour in this figure legend, the reader is referred to the web version of this article.)

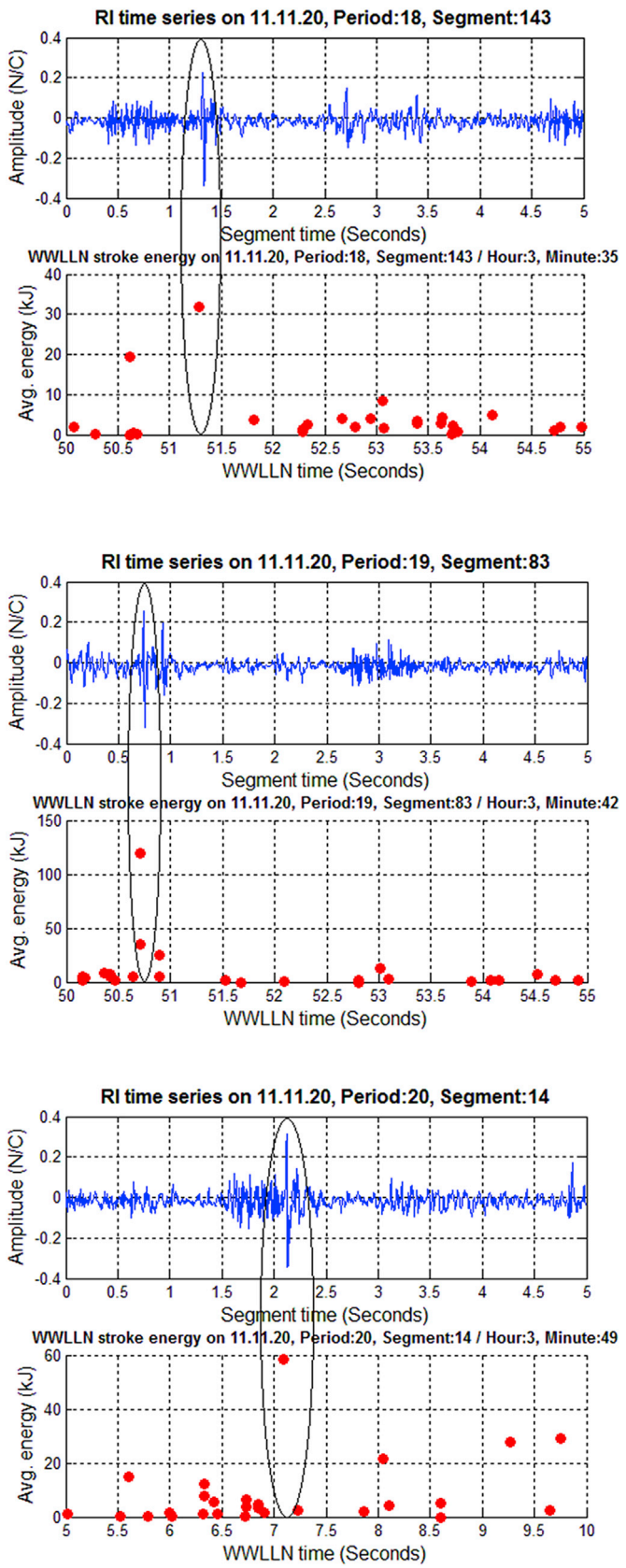

Fig. 8. The sprite event and the corresponding WWLLN-computed average VLF energy of 32 kJ. The black ellipse highlights the causative Q-burst detected in the ELF data as well as by the WWLLN. b: The sprite event and the corresponding WWLLN-computed average VLF energy of 120 kJ. The black ellipse highlights the causative Q-burst detected in the ELF data as well as by the WWLLN. c: The sprite event and the corresponding WWLLN-computed average VLF energy of 59 kJ. The black ellipse highlights the causative Q-burst detected in the ELF data as well as by the WWLLN.

~50–100% increase in PSD (red color PSD) than the background value (blue color PSD). All the higher modes also show significant increase in PSD due to the transient. The PSD shape in the 1st SR mode shows no difference between transient and no transient (background). It is to be noted that we lack knowledge on the origins of the offending transients. Furthermore, there appears to be two transients within the 1 s segment. So, it is difficult to say why different modes are aliased to different degrees. The third event is shows in Fig. 9c. Due to the transient, the first mode PSD becomes ~100% larger (red color PSD) than the background value (blue color PSD). All the higher modes also show significant increase in PSD due to the transient.

In summary, for all three cases selected for the present study, the transients clearly alias the 5-s background spectra in increasing the first and/or second mode intensity. The common feature is that all the higher order modes above the third mode show increased intensity compared to the background spectra.

The same analysis is now performed on a 1-min time series segment that initially does not include the transient. Then the transient is included for an overall duration of one additional second. The analysis is shown in Fig. 10a, b and c. No aliasing over the 1-min time period is discernible. This finding indicates that the selected transients may not be of sufficient intensity to alias over 1 min even if they are capable of aliasing over 5-s segments.

We now present the results of a very-strong (~200 CSD) transient event that showed evidence for eight circumnavigations of the globe, detected at both BLK and NCK locations. For this event, there was no reported sprite. We analyze the transient detected at the BLK station with a CSD of 207 over 5-s segments (207 CSD, Fig. 3B upper panel, period 37, and segment# 54). The result is shown in Fig. 11. Due to the very-strong transient, the first mode PSD becomes ~10% larger (red color PSD) than the background value (blue color PSD), thus showing appreciable aliasing for a single Q-burst event over a 12-min period. All the higher modes also show increase in PSD due to the presence of one very-strong transient in one 5-s segment.

5. Discussion

The analysis of three selected Q-bursts correlated with documented sprite events show that the intensities of these events do not exceed 16 CSD over 5-s intervals. So, we can discern an aliasing effect over 5-s intervals, but when the time interval is extended to 1 min, the aliasing becomes undetectable. Since the events are below 16 CSD, it is unlikely that they would have discernible footprints in the 12-min background spectra. However, a very-strong transient of 207 CSD is capable of aliasing the background SR spectra over a longer time period that is commonly used to extract the SR spectral parameters by a fitting method named as Isolated Lorentzian (I-LOR) (Mushtak and Williams 2009).

It is to be noted that the CSD criteria pertain to strong Q-bursts that have sufficient energy within the time domain from which we compute the background spectrum, so that it can alias the background spectra over that time domain. The criteria is first applied to a 5-s segment to test if it can significantly (above 16 CSD) alias the 5-s spectrum, and if so, the complete 5-s segment is discarded from the average FFT of 144 segments. In this way, we include only those 5-s segments within a 12-min period that contain lightning strokes having ELF intensities comparable to the SR background (irrespective of whether those lightning strokes manifest themselves as Q-bursts, but not having sufficient energy to change the background spectrum significantly).

The stabilization diagram (Fig. 5) clearly shows that within an amplitude window of the CSD of around 6–17, the modal parameters are unaffected by the CSD selection criteria. If the transient amplitude were greater than a threshold value, severe aliasing took place especially in the modal frequency so that the SR modal background parameters over 5-s intervals were affected. It is to be noted that for a selection threshold below 5 CSDs, the modal parameter computations also shows destabilization and becomes 'underrepresented'. This means, below 5 CSDs, we

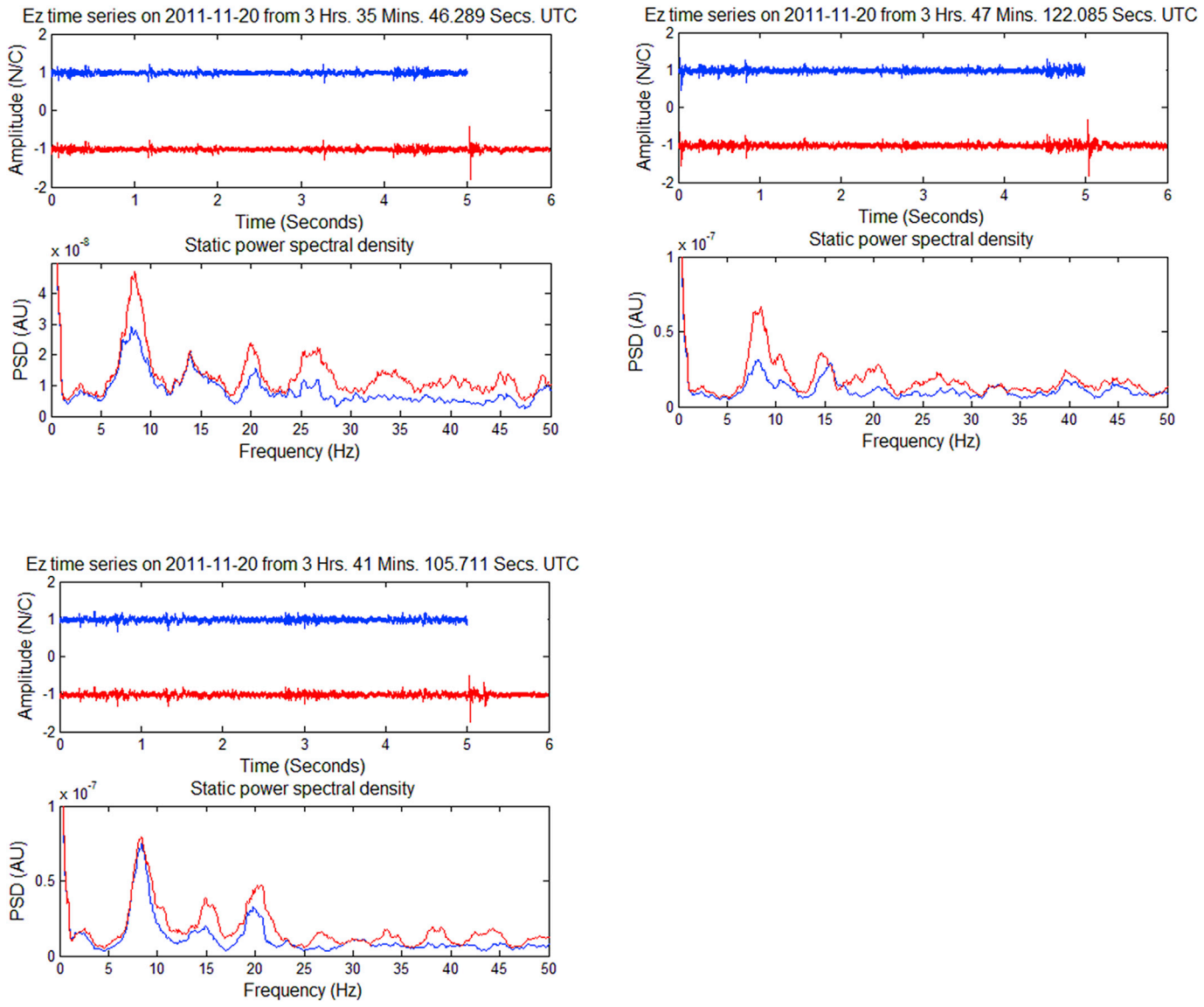

Fig. 9. a: Comparison of 5-s and 6-s segment time series and spectral character for the first transient event (Table 1). The 5-s (blue color) and 6-s (red color) time series are shifted by one unit in vertical scale for better visibility. Due to the transient, the first mode PSD becomes ~50% larger (red color PSD) than the background value (blue color PSD). Higher order modes (above the third mode) exhibit greater PSD compared to the background spectra. b: Comparison of 5-s and 6-s segment time series and spectral character for the second transient event (Table 1). The 5-s (blue color) and 6-s (red color) time series are shifted by one unit in vertical scale for better visibility. Due to the transient, the second mode shows a shift in frequency and ~50–100% increases in PSD (red color PSD) relative to the background value (blue color PSD). All the higher modes also show significant increases in PSD due to the transient. c: Comparison of 5-s and 6-s segment time series and spectral character for the third transient event (Table 1). The 5-s (blue color) and 6-s (red color) time series are shifted by one unit in vertical scale for better visibility. Due to the transient, the first mode PSD (red color PSD) remains same compared to the background value (blue color PSD). All the higher modes also show significant increases in PSD due to the transient. (For interpretation of the references to colour in this figure legend, the reader is referred to the web version of this article.)

start to remove the background components also and thus it affects the modal parameters. Above 16 CSDs, we start to include large transients and thus again spoil the background character. The preferred interval of stabilization is found in a range of CSD thresholds between these two extremes.

It is also to be noted that a moderate transient with respect to the 16 CSD criterion is around 40 CSDs and for a strong transient, it is around 200 CSD (Fig. 3). In comparison to that, the three present cases involving documented sprites have modest amplitudes, much less than 16 CSDs. So, they might not have sufficient intensity even in a 5-s window to strongly alias the background spectra, but still show some indication of aliasing.

In this context, one question that must be addressed is: can 16 CSDs be a universal threshold for aliasing of the SR background by Q-burst transients? This can be addressed by considering a simple calculation involving the energy associated with the background and transients. Let us assume A_B = amplitude of background signal, A_Q = amplitude of Q-burst signal, T_B = duration of background segment used to compute FFT and T_Q = duration of Q-burst transient.

We assume that when the spectral energy of the Q-burst transient is comparable to the spectral energy of the background signal, we will then have appreciable interference problems (spectral aliasing of background signal). Since spectral energy is proportional to the square of amplitude, this condition for major interference with the background spectrum amounts to

$$\begin{aligned} A_B^2 T_B &= A_Q^2 T_Q \\ A_Q^2 \big/ A_B^2 &= T_B / T_Q \end{aligned} \tag{1}$$

Now, if we take a 12-min window to compute the background FFT, and assuming that the Q-burst transient shows eight round trips around the world (Fig. 1B upper panel), this ratio of intensities can be evaluated as the ratio of times:$12(60)/1.04 \approx 690$, where the number 1.04 s comes

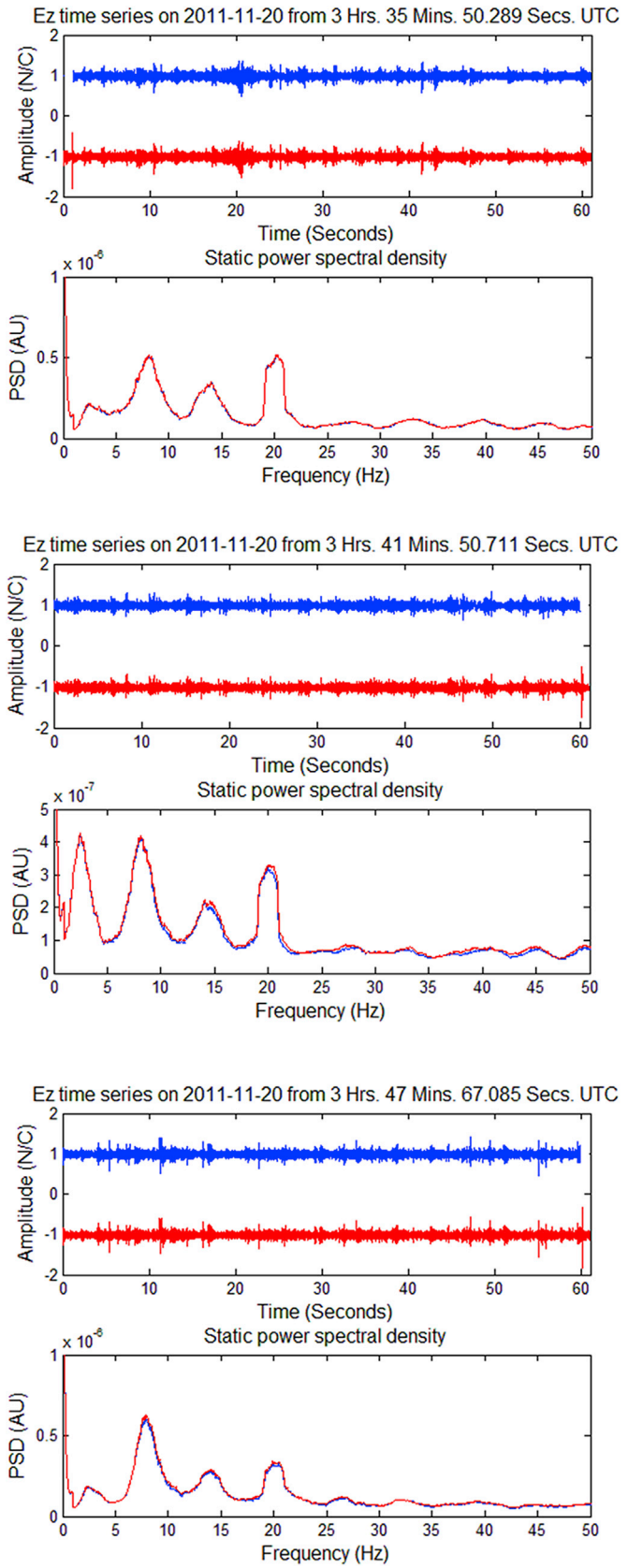

Fig. 10. a: 60-s and 61-s segment time series and power spectrum for the first event (Table 1). The 60 s (blue color) and 61-s (red color) time series are shifted in vertical scale to for better visibility. No aliasing over the 1-min time period is discernible in the PSD. b: 60-s and 61-s segment time series and power spectrum for the second event (Table 1). The 60-s (blue color) and 61-s (red color) time series are shifted in vertical scale to for better visibility. No aliasing over the 1-min time period is discernible in the PSD. c: 60-s and 61-s segment time series and spectrum for the third event (Table 1). The 60-s (blue color) and 61-s (red color) time series are shifted in vertical scale to for better visibility. No aliasing over the 1-min time period is discernible in the PSD. (For interpretation of the references to colour in this figure legend, the reader is referred to the web version of this article.)

from eight round trips of the wave around the world considering a single circumnavigation time of 130 ms.

The result of this rough calculation is within a factor of three of the number 207 CSD (standard deviations of the background intensity) for the super-transient studied here. For the present investigation, the sprite correlated Q-burst CSDs over 5-s intervals are found to be between 1.5 and 16, thus aliasing the background spectra in 5-s intervals. So, over a 12-min period, 16 CSDs appears to be a reliable threshold for aliasing of the SR background by Q-burst transients.

Another important issue arising in the present context is how often we would get a spectral aliasing if we did not clean these events from our data before performing FFTs. The statistics in Fig. 12 show that Q-burst (~200 CSD) events are indeed rare in their occurrence. So, for the SR background sanitation, their sole relevance may not be highly influential given their frequency of occurrence with respect to the aliasing in the modal intensity. But when we examine the effect of these Q-bursts on modal frequency, we note that one may not need large Q-bursts events (~200 CSD) for such aliasing.

For example, the CSD statistics show that above 16 CSD, although the number of 5-s segments decays very rapidly, there are significant numbers of 5-s segments above 16 CSD (total 58 on 5th January 2009), that could significantly alias the modal frequency in SR spectra. One such evidence is presented in Fig. 5A (period 39, segment 134). We clearly note the deviation from the stabilization interval in the modal frequency up to ~0.3 Hz, where the dynamic range of the diurnal variation of the modal frequency is 1–1.5 Hz around the mean value. This aliasing occurs due to the presence of only two 5-s segments having 36 CSDs (segment 134) and 18 CSDs (segment 85), respectively. This is around 20% deviation in the modal frequency if only two 5-s segments within 16–40 CSDs are included in the computation of the 12-min background spectra. As we deal with 120 12-min spectra over an entire day for the extraction of background SR parameters, that statistic of 5-s segments above 16 CSD threshold shows that around 20% of 12-min spectra (24 12-min integrated spectra) could be affected by these transients, especially through frequency aliasing. The effect of aliasing on the intensity for these relatively smaller CSD segments may not be evident in 12-min spectra, but only when we deal with very large transients of the order of 200 CSD. So, the aliasing in modal frequency is important at a much lower level of CSD and thus should be taken into consideration in SR data sanitation.

A simple arithmetic calculation supports the above discussion. We have 144 segments, 5 s long, to make a 12-min block. Suppose for simplicity that the mean frequency in the 143 segments was f_o and all of those segments are 1 CSD. But in a single 5 s block with a 16 CSD event, the transient source was drastically displaced from the background source location and its mean frequency was shifted to $f_o + \Delta f$. Then the overall mean frequency for the full 12 min block would be (when normalized to total energy received = 143 + 16)

$$<f> = (143\ f_o + 16\ (f_o + \Delta f))/\ (143 + 16) \quad (2)$$

Solving for $<f>/f_o$ yields $<f>/f_o = 1 + 16/159\ \Delta f/f_o$. If $\Delta f/f_o = 0.1$ (i.e., 10%), $<f>/f_o = 1.01$.which amounts to a 1% alias in frequency, which is still observable and important. This explains how a single transient event with 16 CSD can alias the frequency appreciably and why values close to 200 CSDs are not needed for frequency aliasing.

The long-standing working hypothesis for this aliasing is that the transients represent the mesoscale lightning "tail" in the diurnal variation, with the background signal coming primarily from the earlier late-afternoon convective activity (of ordinary thunderstorms). The presence of the mesoscale "tail" may rest on the meteorological tendency for late afternoon convective scale thunderstorms to amalgamate into late

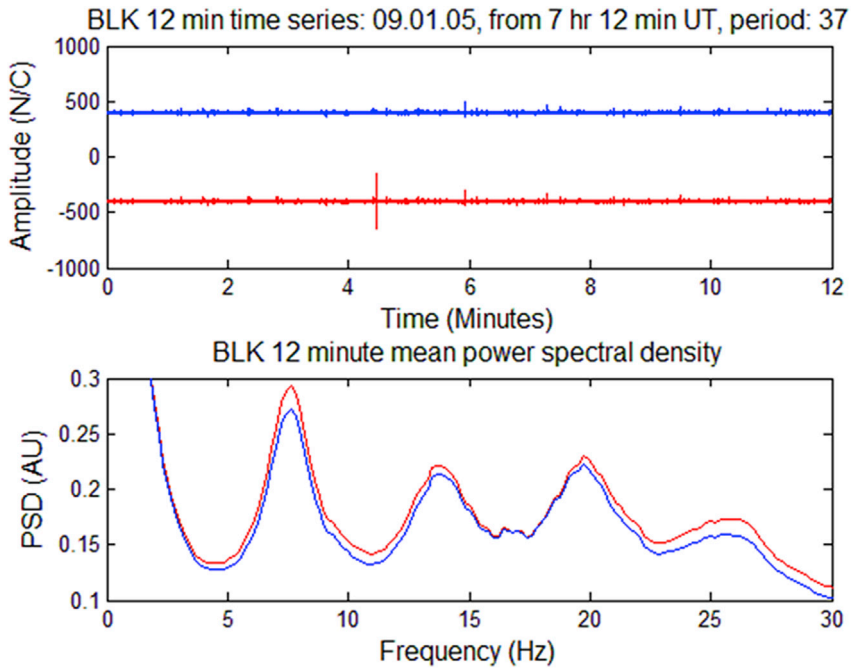

Fig. 11. 12-minute (720 s) segment time series and spectral character for a very-strong transient event ((207 CSD, Fig. 1B upper panel), period 37, segment# 54. The 720 s time series without the 5-s segment# 54 containing the very-strong transient event (blue color) and with the very-strong transient event (red color) are shifted in vertical scale to for better visibility. Due to the very-strong transient, the first mode PSD becomes ~10% larger (red color PSD) than the background value (blue color PSD), thus showing appreciable aliasing for a single Q-burst event over a 12-min period. All the higher modes also show increase in PSD due to the presence of one very-strong transient within a 5-s segment. (For interpretation of the references to colour in this figure legend, the reader is referred to the web version of this article.)

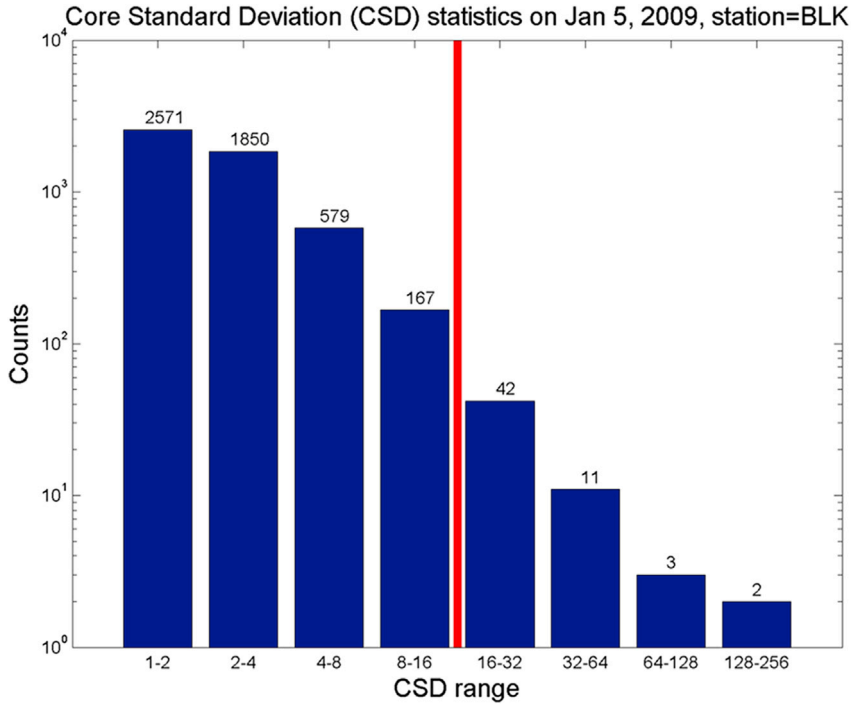

Fig. 12. The statistics of 5-s segment Core Standard Deviation (CSD) on 5th January 2009 at the Belsk (BLK) station. Actual counts are indicated at the top of each bar of the histogram. At or above 1 CSD, a total of 5225 5-s segments are found out of a total 17280 5-s segments in a day. The left hand side of the vertical line (at 16 CSD) denotes the 'background' segment, whereas the right hand side of the line represents the 'non'-background' segment of the SR spectral content. (For interpretation of the references to colour in this figure legend, the reader is referred to the web version of this article.)

evening mesoscale convective systems. The former entities are excellent producers of the background SR signal, whereas the latter ones are good producers of mesoscale lightning flashes with exceptionally energetic transients of the kind shown to be "spoilers" of the experimental background results. It is worth mentioning that maybe there could be some fundamental interaction between background and transient phenomena, such as an accumulation of charge imbalance that leads to the very-strong transients. This interaction also deserves a thorough study.

It is worth mentioning that the present work deals with both "cleaning data" as well as "detecting TLEs but with an emphasis on sanitizing the SR data. The detection of TLE's with the CSD method combined with hyperbolic ranging is our future objective that might be achieved by first picking up the time of arrival from the peak amplitude within the 5-s segments that exceed a fixed CSD threshold and then using a TOA method to locate the TLE events (Yamashita et al., 2011).

6. Concluding remarks

Based on the analysis, we conclude that the Q-bursts associated with three verified sprites do not modify the SR background spectra completely, but can modify the spectral content, and thereby detrimentally alias the spectral input to a background inversion method. Though the present three sprite-generating events did not have sufficient energy to alias the longer time series data, one Q-burst transient of substantially larger amplitude was shown to alias the spectrum derived from the 12-min interval in which it was found. On examination of the occurrence statistics of the strong Q-bursts (~200 CSD), it is found that their occurrence rate is not high enough to alias the modal intensity of the SR spectra, but the modal frequency could be affected by much smaller transients having CSD in the range 16–40. It is expected that the CSD methodology could be effectively used to determine the time of arrival of the global transients and then to detect TLEs globally with a small number of networked stations. Such a procedure would be especially valuable during daylight conditions, when optical measurements of TLEs are not generally feasible and when the amplitude of the ELF transient may be exceptional (Stanley et al., 2000).

Acknowledgments

We cordially thank Robert Holzworth for providing the WWLLN lightning locations and average VLF energy data for this study. We also thank Oscar van der Velde and Serge Soula for providing us with optical images of the sprites detected from the Ebro Delta in northeastern Spain and Mariusz Neska for the provision of the Belsk data. The work is partially supported by the USIEF-India Fulbright-Nehru, UGC Raman post-doctoral fellowship programs and by the generous support from the Grainger Foundation, USA. The contribution of József Bór was supported by the János Bolyai Research Scholarship of the Hungarian Academy of Sciences (BO/00651/13/10h). The work of József Bór and Gabriella Sátori was supported by the National Research, Development and Innovation Office, Hungary-NKFIH, K115836. The work of Joan Montanyà was supported by research grants from the Spanish Ministry of Economy and Competitiveness and the European Regional Development Fund: ESP2013-48032-C5-3-R, and ESP2015-69909-C5-5-R. The analysis of the datais partially supported by DST-FIST fund reference Ref.SR/FST/PSI-191/2014, Government of India. This investigation was initiated by Vadim Mushtak (deceased), and its findings are dedicated to his memory.

References

Betz, H.D., Schmidt, K., Oettinger, P., Wirz, M., 2004. Lightning detection with 3-D discrimination of intracloud and cloud-to-ground discharges. Geophys. Res. Lett. 31, L11108.

Boccippio, D.J., E. Williams, E., Heckman, S.J., Lyons, W.A., Baker, I., R. Boldi, R., 1995. Sprites, ELF transients and positive ground strokes. Science 269, 1088–1091.

Cummer, S.A., Frey, H.U., Mende, S.B., Hsu, R.R., Su, H.T., Chen, A.B., Fukunishi, H., Takahashi, Y., 2006. Simultaneous radio and satellite optical measurements of high-altitude sprite current and lightning continuing current. J. Geophys. Res. 111, A10315.

Guha, A., Williams, E., Boldi, R., Satori, G., Nagy, T., Montanyà, J., Ortega, P., 2014. Schumann resonance spectral characteristics: a useful tool to study Transient Luminous Events (TLEs) on a global scale. In: Proceedings of the XV International Conference on Atmospheric Electricity, June 15–20, Norman, Oklahoma, U.S.A.

Hobara, Y., Hayakawa, M., Williams, E.R., Boldi, R., Downes, E., 2006. Location and electrical properties of sprite-producing lightning from a single ELF site, in Sprites, Elves and Intense Lightning Discharges. In: Fullekrug, M., Mareev, E.A., Rycroft, M.J. (Eds.), NATO Science Series, II. Mathematics, Physics and Chemistry, vol. 225. Springer, p. 398.

Huang, E., Williams, E.R., Boldi, R., Heckman, S., Lyons, W., Taylor, M., Nelson, T., Wong, C., 1999. Criteria for sprites and elves based on Schumann resonance observations. J. Geophys. Res. 104, 16943–16964.

Hutchins, M.L., Holzworth, R.H., Rodger, C.J., Brundell, J.B., 2012. Far-Field power of lightning strokes as measured by the world wide lightning location network. J. Atmos. Ocean. Technol. 29, 1102–1110.

Hutchins, M.L., Holzworth, R.H., Virts, K.S., Wallace, J.M., Heckman, S., 2013. Radiated VLF energy differences of land and oceanic lightning. Geophys. Res. Lett. 40, 1–5.

Mushtak, V.C., Williams, E.R., 2009. An improved Lorentzian technique for evaluating resonance characteristics of the Earth-ionosphere cavity. Atmos. Res. 91, 188–193.

Mushtak, V., Williams, E.R., Boldi, R., Nagy, T., 2010. On estimation strategies in an inverse ELF problem. Geophys. Res. Abstr. 12, EGU2010–14625. EGU General Assembly 2010.

Mushtak, V., Williams, E., 2011. On use of statistical information in the inverse ELF problem for global 393 lightning. In: XIV International Conference on Atmospheric Electricity, August 08-12, Rio de Janeiro, 394 Brazil.

Mushtak, V.C., Williams, E.R., Neska, M., Nagy, T., 2012. On sanitizing background Schumann resonance observations from strong transient events for inversion calculations. In: 1st TEA-IS Summer School, Malaga, Spain, June.

Nickolaenko, A.P., Hayakawa, M., Hobara, Y., Q-Bursts, 2010. Natural ELF radio transients. Surv. Geophys. 31 (4), 409–425.

Ogawa, T., Tanaka, Y., Yasuhara, M., Fraser-Smith, A.C., Gendrin, R., 1967. Worldwide simultaneity of occurrence of a Q-type ELF burst. J. Geomag. Geoelec. 19, 377–384.

Price, C., 2016. ELF electromagnetic waves from lightning: the Schumann resonances. Atmosphere 7 (9), 116.

Stanley, M., Brook, M., Krehbiel, P., Cummer, A.A., 2000. Detection of daytime sprites via a unique sprite ELF signature. Geophys. Res. Lett. 27 (6), 871–874.

van der Velde, O.A., Montanyà, J., Soula, S., Pineda, N., Mlynarczyk, J., 2014. Bidirectional leader development in sprite-producing positive cloud-to-ground flashes: origins and characteristics of positive and negative leaders. J. Geophys. Res. Atmos. 119, 12755–12779.

Williams, E.R., Castro, D., Boldi, R., Chang, T., Huang, E., Mushtak, V., Lyons, W., Nelson, T., Heckman, S., Boccippio, D., 1999. The relationship between the background and transient signals in Schumann resonances. In: 11th International Conf. On Atmos. Elec., Guntersville, Alabama, June 7–11.

Yamashita, K., Takahashi, Y., Sato, M., Kase, H., 2011. Improvement in lightning geolocation by time of arrival method using global ELF network data. J. Geophys. Res. 116, A00E61.